Synthesis and characterization of halogen-containing aryl amide polymer-clay nanocomposites

Ali DELİBAŞ[*], **Murat ALPARSLAN**

Department of Chemistry, Faculty of Sciences and Arts, Bozok University, Yozgat, Turkey

Abstract: Synthesized N-(4-bromophenyl)-2-methacrylamide (BrPMAAm) and N-(4-fluorophenyl)-2-methacrylamide (FPMAAm) monomers were polymerized via free radical polymerization. Montmorillonite-containing raw clay (NaMT) was purified to obtain pristine clay (SMT). XRF results of the SMT sample showed that sodium amount increased and so it is sodium montmorillonite. Using the SMT and organic surfactant hexadecyltrimethylammonium bromide (CTAB), organoclay (OSMT) was synthesized. d_{001} interlayer distances were 1.4967 nm and 2.0439 nm for SMT and OSMT, respectively. Composites of BrPMAAm and FPMAAm monomers were obtained using 2%, 4%, 6%, and 10% organoclay by in situ polymerization. Molecular weights for poly(BrPMAAm), poly(BrPMAAm)-10%OSMT, poly(FPMAAm), and poly(FPMAAm)-10%OSTM were 91,300, 31,300, 17,400, and 23,700, respectively. Thermal properties of the nanocomposite were also developed when compared to the pure homopolymer. The beginning thermal decomposition temperature of nanocomposites was shifted to higher temperature. An exfoliated structure was found for the nanocomposites.

Key words: Polymeric composites, thermal analysis, organoclay, aryl amide polymer, montmorillonite

1. Introduction

In the last two decades, for preparing hybrid materials, polymers on the organic side and clays on the inorganic side for nanocomposites have attracted great interest, both in industry and in academia. The fact that nanocomposite materials display significant improvement in the properties of materials when compared with original polymer or conventional micro- and macrocomposites has resulted in a considerable increase in studies in this area.[1−4] Polymers and polymer nanocomposites have been extensively preferred to replace the traditional metals and ceramics in microelectronic packaging, coatings, aerospace, automotive, food packaging, and biomedical applications, because of their superior or matching properties and lower production costs.[5−7]

Montmorillonite is nowadays the most preferred commercial layered silicate as nanofiller in the preparation of nanocomposites. However, the hydrophilic nature of montmorillonite limits its compatibility with organophilic polymers. Thus, clay has been rendered hydrophobic to make montmorillonite compatible with organophilic polymer. Due to the presence of exchangeable metal cations like Na^+, Li^+, and Ca^{2+}, the modification of montmorillonite can be easily achieved with alkyl ammonium salts to form organo-montmorillonite.[8−11] The preparation of clay-based nanocomposites is achieved by several methods: solution exfoliation, melt intercalation, and in situ polymerization. In the in situ polymerization method, the monomer is used directly as a solubilizer for swelling the layered silicate. Polymerization occurs in the intercalated clays.[1,3,12,13]

---

[*]Correspondence: ali.delibas@bozok.edu.tr

Poly(phenylmethacrylate) and poly(phenylmethacrylamide) polymers have high tensile strength, thermal stability, and glass transition temperature compared with their acrylates polymer because of the presence of the methyl group and phenyl group on the main chain. Brominated acrylates are more thermally stable than other acrylates.[14−16] Although there is a broad range of literature covering the acrylate nanocomposites, there are few studies focused on phenymethacrylamide and its nanocomposite.[17−19]

In addition, halogen-including aryl amide polymers have flame retardancy, and high tensile and thermal properties, and it is noteworthy that clay nanoparticles as filler enhance flame retardancy, and mechanical and thermal properties. The combination of clay and aryl amide polymers could exhibit a synergistic effect on the properties mentioned above.[20]

The aim of the present study was the synthesis of halogen-containing aryl amide polymer-clay nanocomposites. Clay was purified and modified with CTAB by using ion exchange to provide better interactions between polymer and clay. FPMAAm and BrPMAAm monomers were synthesized and their nanocomposites were prepared with organophilic clay by in situ free-radical polymerization. Clay-associated changes in thermal properties, morphology, and molecular weights were discussed.

2. Results and discussion

2.1. XRD analysis

As seen from the XRD patterns in Figure 1a, $d_{001} = 1.4967$ nm for the SMT. Chemical compositions of the natural clay sample (NaMT) and purified clay (SMT) were determined by X-ray fluorescence (XRF) analysis. According to the XRF results (Table 1), after the purification procedure the sodium content of the purified clay increased from 0.80% to 0.98% as Na_2O. XRD and XRF results indicated that the purification procedure was effective and the clay obtained was rich in Na montmorillonite.[21]

In Figure 1b, the XRD pattern of OSMT, $d_{001} = 2.0439$ nm. A decrease in the 2θ value and an increase of 0.54 nm in d_{001} interlayer distance showed that modification of SMT with hexadecyltrimethyl ammoniumbromide (CTAB) was accomplished and the clay was turned into organophilic form. The verification of cationic surfactant CTAB inside the SMT was also done by FTIR.[19,22,23]

The diffraction patterns of the OSMT, poly (BrPMAAm)/organoclay, and poly (FPMAAm)/organoclay nanocomposites are given in Figure 1c and 1d. The primary silicate reflection at nearly $2\theta = 5°$ in the organoclay corresponds to layer spacing of 2.0439 nm. For the poly(BrPMAAm)/organoclay samples (Figure 1c), there were no sharp reflections below $2\theta = 10°$ in the nanocomposites, which was attributed to exfoliation of the organoclay in the nanocomposites. In Figure 1d, for the poly(FPMAAm)/organoclay nanocomposite-4%, a diffraction peak was observed in the $2\theta = 6.2$ value. This may result from the overlap of some organoclay and polymer chain layers. It indicated the existence of an intercalated nanocomposite structure. However, loading 10% OSMT composite exhibited almost totally exfoliated structures.[19,23]

2.2. FTIR analysis

In Figure 2e, the bands at 1009–1020 cm^{-1}, 514 cm^{-1}, and 786 cm^{-1} are Si–O in plane stretching, Si–O–Al deformation band, and Mg–Al–OH bending vibrations, respectively, and the bands at 2952 and 2923 cm^{-1} show aliphatic C–H stretching of CTAB. These main bands confirmed the organoclay structure.[24,25]

Table 1. XRF results for NaMT and SMT.

NaMT			SMT		
L.O.I.: 6.30%			L.O.I.: 4.53%		
Constituent	(%)	Error (%)	Constituent	(%)	Error (%)
1 SiO_2	73.6041	0.2	1 SiO_2	85.1817	0.2
2 Al_2O_3	12.6314	0.05	2 Al_2O_3	7.2443	0.04
3 Fe_2O_3	1.9546	0.01	3 Na_2O	0.9754	0.02
4 CaO	1.8302	0.02	4 Fe_2O_3	0.7834	0.006
5 MgO	1.5547	0.009	5 MgO	0.7756	0.007
6 K_2O	0.8162	0.009	6 K_2O	0.1513	0.005
7 Na_2O	0.7984	0.01	7 CaO	0.0986	0.004
8 TiO_2	0.1478	0.005	8 TiO_2	0.0875	0.004
9 Cl	0.1866	0.005	9 Cl	0.0212	0.002

L.O.I.: Losses of ignition.
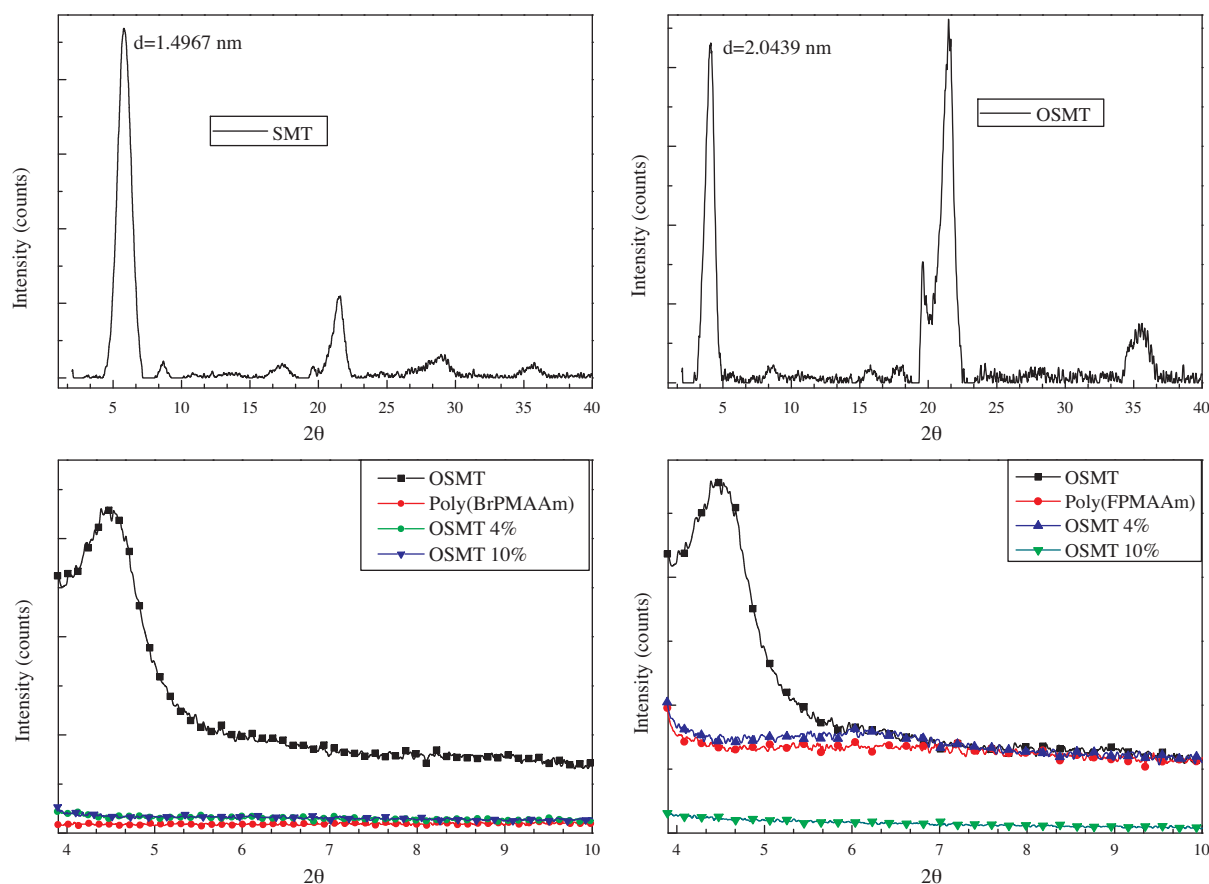
Figure 1. XRD pattern of a) SMT b) OSMT c) poly(BrPMAAm) nanocomposites d) poly(FPMAAm) nanocomposites.

FTIR spectra of polymers and composites exhibited specific bands for polymer and clay (Figure 2a–2d). For the poly(BrPMAAm) and poly(FPMAAm), while bands at 3330 cm^{-1} (–NH), 3030 cm^{-1} (aromatic =C–H), 2960 cm^{-1} (aliphatic –C–H), and 1660 cm^{-1} (amide –C=O) were observed, in the composites adding to these bands 1045 cm^{-1} (Si–O stretching peak) and 460 cm^{-1} (Si–O–Si deformation band) were determined with the increasing OSTM content.
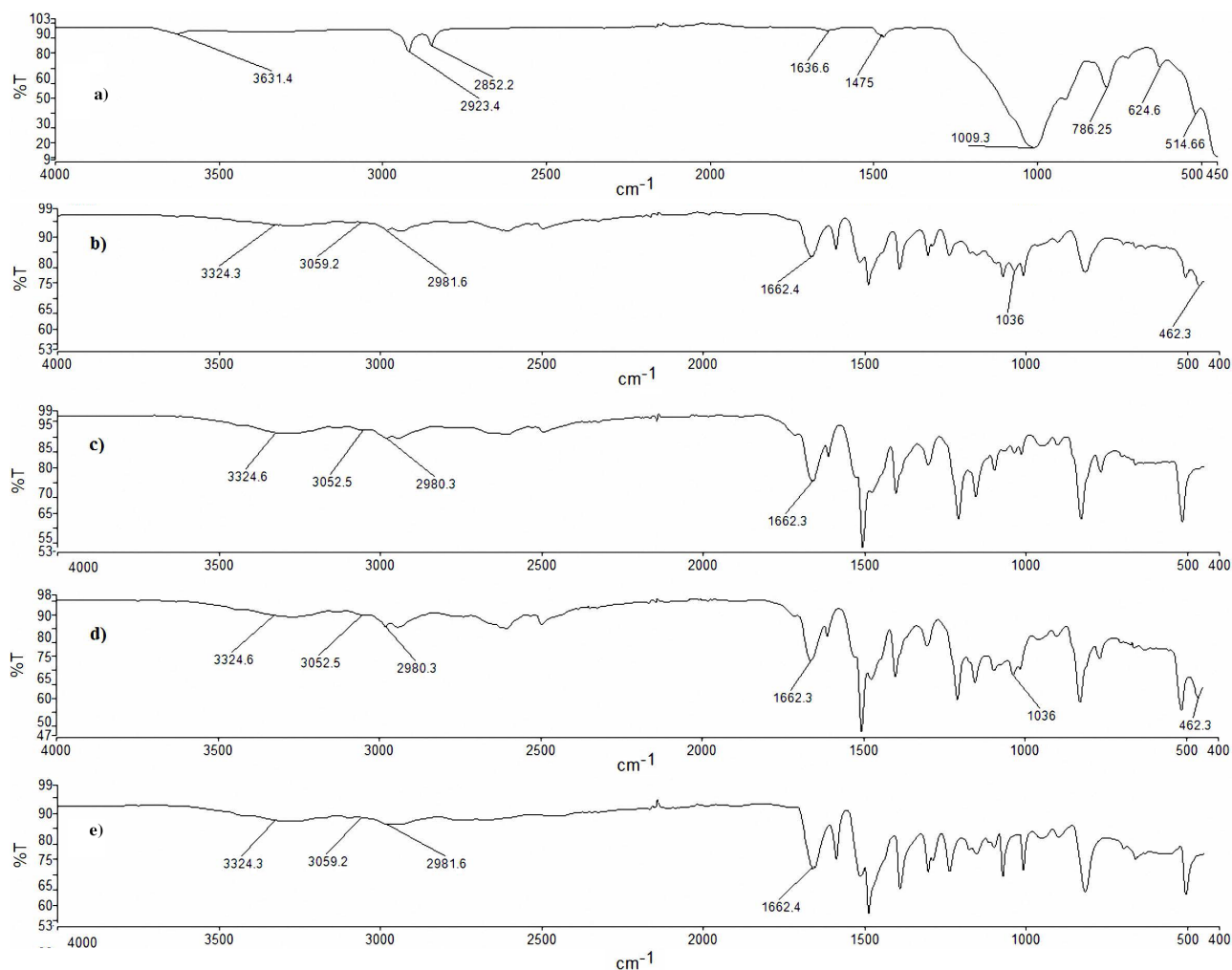
Figure 2. FTIR spectra of a) poly(BrPMAAm) b) poly(BrPMAAm)/OSMT(10%), c) poly(FPMAAm)
d) poly(FPMAAm)/OSMT (6%) e) OSMT.

2.3. SEM and thermal analyses

Scanning electron microscopy images were used for further characterization of nanocomposites. The images in
Figure 3 show the changes in morphology of the nanocomposites. As seen in the SEM images, the clay was
dispersed in the polymer matrix and it became noticeable with the increase in the clay content.

The thermal characterization of the polymers was carried out by thermogravimetric analysis (TGA) and
differential scanning calorimetry (DSC) under nitrogen atmosphere. All the polymers and nanocomposites
underwent multistage decomposition, as shown in Figure 4. Both TGA graphics were investigated and initial
weight loss temperature of nanocomposite was increased to compare it with the homopolymer TG curves.
Moreover, residual mass amount was increased in nanocomposite samples (Table 2). The increase in residual
mass amount (char yield) could imply a reduction in the polymer's flammability.[17] This showed that the
thermal stability of the poly(BrPMAAm) and poly(FPMAAm) was improved using OSMT and OSMT clays
incorporated into the polymer matrix. The increase in thermal stability is due to the silicate layer dispersed in
the polymer matrix causing physical protection. This has a positive effect on the decomposition barrier and char
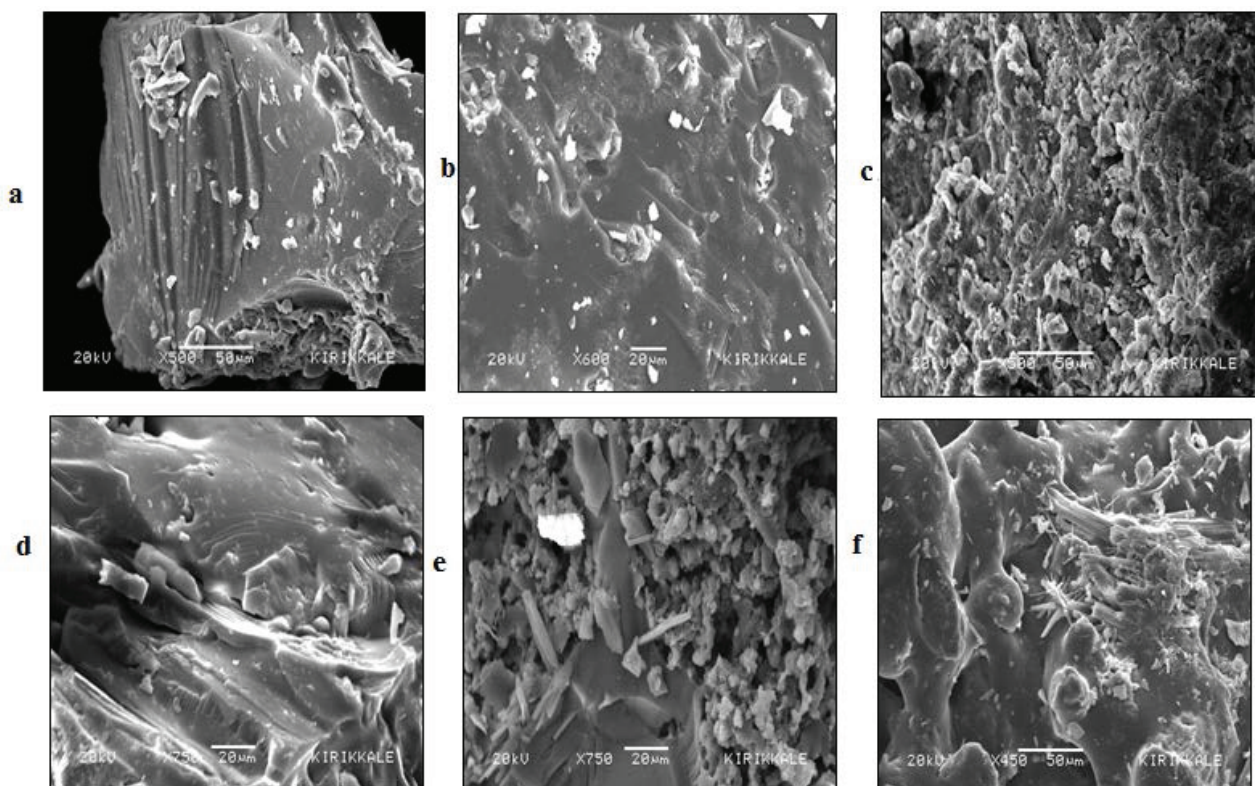
Figure 3. SEM images of homopolymers and nanocomposites a) poly(BrPMAAm), b) poly(BrPMAAm)/2%OSMT c) poly(BrPMAAm)/10%OSMT d) poly(FPMAAm), e) poly(BrPMAAm)/2%OSMT f) poly(BrPMAAm)/6%OSMT.

formation.[9] As seen in Table 2, T_g values for poly (BrPMAAm) and its composites were quite high, whereas all nanocomposites showed values of both T_g and T_m (in Figure 5). However, T_g values decreased as OSTM content increased and T_m values increased as OSTM content increased. A decrease in T_g values usually occurs in highly filled and/or intercalated nanocomposites.[26] The second endothermic peak for BrPMAAm nanocomposites observed can be attributed to the existence of a new crystal phase caused by polymer or clay[27], or second T_{g2} point of BrPMAAm nanocomposites. Yılmaz observed two different endothermic transitions in his studies.[26] While poly(FPMAAm) displayed both T_g and T_m, its nanocomposites exhibited only a T_g value (in Figure 6). Nanocomposite including 6% OSTM showed a higher and one point T_g value. This can be explained by the intercalated structure observed in the XRD pattern.

2.4. GPC analyses

Molecular weights of homopolymer and clay-removed polymers were determined using GPC and the results are given in Table 2. Clay removal was performed by solving the samples in DMF again; they were later centrifuged at 5000 rpm and filtered with a 5-μm Teflon filter. The Mw of BrPMAAm homopolymer is greater than that of FPMAAm homopolymer. Molecular weight has an influence on glass transition temperature and obviously is seen in the results of 157.3 and 114.2 °C for BrPMAAm and FPMAAm, respectively.[14] The bigger difference between the Mw of BrPMAAm and FMAAm could be explained by using the Br-styrene and F-styrene propagation rate constant in which Br-Sty has a bigger k_p value than F-Sty.[28] Furthermore, flour is more active than bromine as a radical, and so flour, like a chain transfer agent, can cause a decrease in the
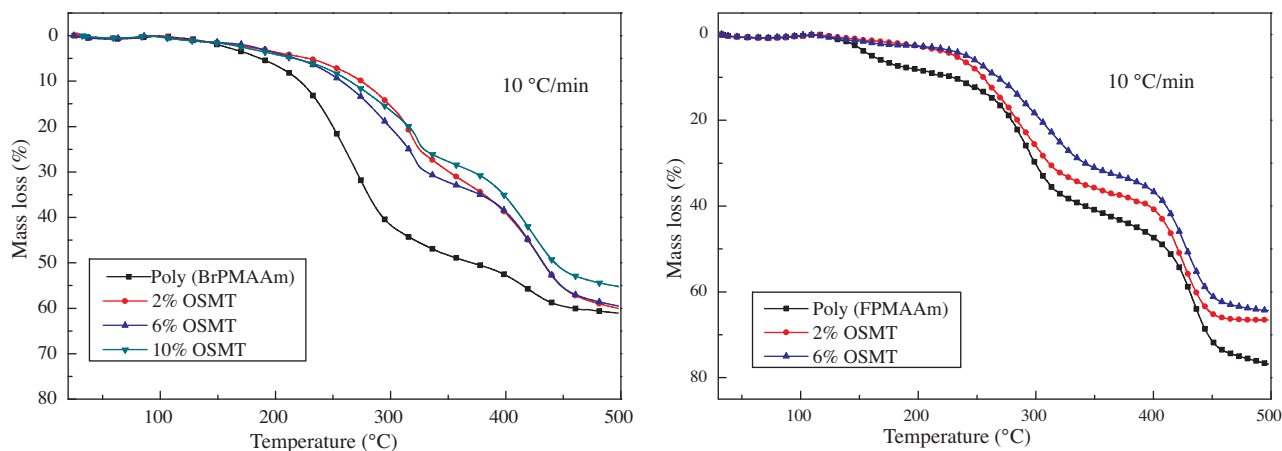
Figure 4. TG curves of the a) poly(BrPMAAm) and its nanocomposites, b) poly(FPMAAm) and its nanocomposites.
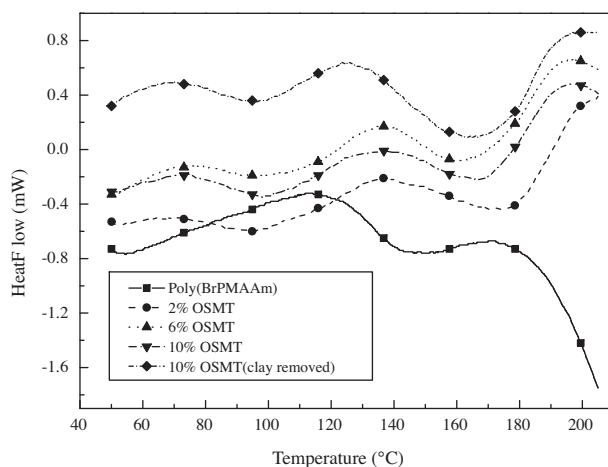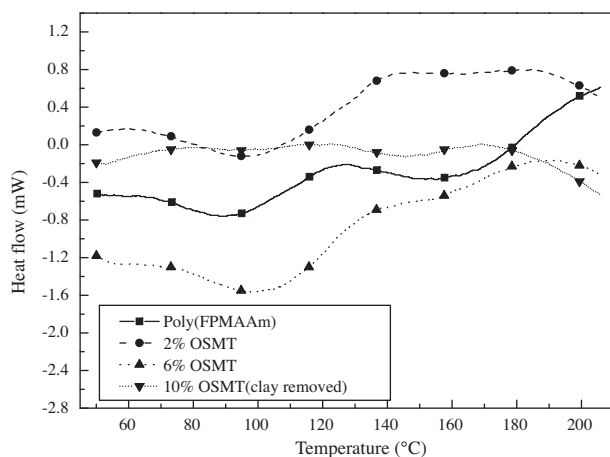

Figure 5. DSC curves of the poly(BrPMAAm) and nanocomposites.

Table 2. Some parameters of polymers and their composites obtained TGA, DSC, and GPC.

Samples	Tg °C	Tm °C	50% weight loss temp. (°C)	Residual mass (%)	M_w/HI
Poly (BrPMAAm)	157.3	-	370.6	39.0	91,300/1.28
2% OSMT-BrPMAAm	128.3	158.0	432.6	40.0	
6% OSMT-BrPMAAm	123.7	182.7	432.4	40.5	
10% OSMT-BrPMAAm	85.6	182.4	442.8	55.2	
10% OSMT- BrPMAAm*	81.2	183.8	-	-	31,300/1.02
Poly (FPMAAm)	114.2	131.5	411.1	23.1	17,400/1.26
2% OSMT-FPMAAm	132.7	148.7	420.6	33.4	
6% OSMT-FPMAAm	123.6	177.7	428.2	35.7	
10% OSMT-PMAAm*	111.3	156.7			23,700/1.10

*Clay removed polymer HI:Heterogenety Index

molecular weight of FPMAAm polymer.[29] In the nanocomposite of BrPMAAm, molecular weight was less than that of the homopolymer of BrPMAAm, but nanocomposite of FPMAAm molecular weight was higher than that of homopolymer of FPMAAm. HI values indicated that the polymerization process is ideal for polymer nanocomposites.

Figure 6. DSC curves of the poly(FPMAAm) and nanocomposites.

3. Conclusions

Natural clay was purified and the CEC value was 110 meq/100 g. Using this pristine clay, SMT, OSMT was synthesized via cation exchange by CTAB. In SMT and OSMT, the interlayer distance was 1.4967 nm and 2.0439 nm, respectively. BrPMAAm and FPMAAm monomers were synthesized and their nanocomposites were prepared successfully and an exfoliated type of nanocomposite was found. Moreover, SEM images showed the clay dispersed in the polymer matrix homogeneously. The thermal behavior of nanocomposites showed that the thermal stability of BrPMAAm and FPMAAm nanocomposites was enhanced by the clay content. Furthermore, after the flame retardancy test, these composites could be used for some special applications due to clay and halogen including aryl amide polymer synergic effect. The composites' molecular weights compared with homopolymers indicate that OSMT exhibited behavior like a chain transfer agent in polymerizations.

4. Experimental

4.1. Material and reagents

Methacryloyl chloride (Alfa Aesar), 4-bromoaniline, 4-floroaniline, hexadecyltrimethyl ammoniumbromide (CTAB), methylene blue, N,N-dimethylformamide (DMF), dichloromethane, diethylether, tetrahydrofurane (THF), triethyl amine (NR_3), and azobisisobutyronitrile (AIBN) (Merck) were used as analytical grade commercial products. The natural clay sample was taken from the Yozgat region, Turkey.

4.2. Characterizations

The IR spectra of all samples were recorded with a PerkinElmer Spectrum Two model instrument in the range of 4000–400 cm^{-1}. XRD analysis of the samples was carried out with a Rigaku D/Max 2200 Ultima-PC using a Cu tube (λ = 1.5405 nm) as the X-ray source. Scanning electron microscope observation was performed with a Jeol JSM 5600 apparatus at 20 kV after gold coating. XRF analysis was performed with a WD-XRF PANalytical-Axios Advanced. Molecular weight of the samples was determined with a Malvern Viscotek Max GPC, calibrated with polystyrene, with a flow rate of 1 mL/min, and THF used as the solvent. Thermal data were obtained using a Setaram Labsys TG-DSC/DTA thermo balance and DSC 131 in nitrogen atmosphere.

4.3. Purification of clay and synthesis of organoclay

Natural raw clay (NaMT) was ground and sieved (200 μm). The ground clay sample was left to dry for 24 h and then chemically purified to remove organic materials and contaminants.[21,30] It was named SMT (pristine montmorillonite). The cation exchange capacity (CEC) of SMT was determined as 110 meq/100 g clay using the methylene blue method. The CEC of montmorillonite ranges between 76 and 120 meq/100 g.[31]

Cationic surfactant hexadecyltrimethyl ammonium bromide (CTAB) was used for the synthesis of organoclay by the well-known ion exchange method. Firstly 5 g of clay was dispersed in 400 mL of ultrapure water for 48 h and the pH of the solution was adjusted to 3 with conc. HCl. CTAB was added to the solution with a CEC more than that of SMT and mixed with a magnetic stirrer at 500 rpm for 24 h. After the precipitation of organoclay, samples were washed several times and centrifuged at 4000 rpm. The organic modified montmorillonite sample was dried at 40 °C and named OSMT.[31,32]

4.4. Synthesis of monomers

FPMAAm and BrPMAAm monomers were synthesized by well-known organic reactions that were described previously in our studies and others.[15,16] FPMAAm and BrPMAAm monomers were synthesized with reactions of 4-bromoaniline (0.1 mol) or 4-floroaniline (0.1 mol) in dichloromethane with methacryloyl chloride (0.11 mol) using triethyl amine (0.3 mol) in an ice bath (0–5 °C). The monomers were recrystallized from a methanol and water mixture.

4.5. Preparation of polymer and polymer nanocomposites

FPMAAm and BrPMAAm monomers were polymerized to obtain homopolymers in DMF using AIBN (1% on mole basis) at 70 °C after solutions were purged with nitrogen. All solutions were poured slowly into the excess diethyl ether to precipitate the polymers. After filtration, the polymers were dried in an oven at 45 °C.

Previously determined (2%, 4%, 6%, 10%) amounts of OSMT were stirred in DMF for 2 h and FPMAAm and BrPMAAm monomers were added to the solution at a concentration of 1 M and stirred together for 2 h again and ultrasonicated for 30 min with a Bandelin Sonorex ultrasonicator in an ice bath. AIBN (1% on mole basis) as an initiator was added to the dispersion and purged with nitrogen for 20 min. The mixture was heated to 70 °C to be polymerized in a water bath for 24 h. After cooling to room temperature, the composites' dispersion was poured into excess of diethyl ether for precipitation. The composite sample was filtered and dried at 45 °C.

Acknowledgment

References

1. Ray, S. S.; Okamoto, M. *Prog. Polym. Sci.* **2003**, *28*, 1539–1641.

2. Paul, D. R.; Robeson, L. M. *Polymer* **2008**, *49*, 3187–3204.

3. Nguyen, Q. T.; Baird, D. G. *Adv. Polym. Tech.* **2006**, *25*, 270–285.

4. Ding, C.; Guo, B.; He, H.; Jia, D.; Hong, H. *Eur. Polym. J.* **2005**, *41*, 1781–1786.

5. Brostow, W.; Dutta, M.; De Souza, J. R.; Rusek, P.; De Medeiros A. M.; Ito. E. N. *Express Polym. Lett.* **2010**, *9*, 570–575.

6. Kaynak, C.; Nakas, G. I.; Isitman, N. A. *App. Clay. Sci.* **2009**, *46*, 319–324.

7. Meneghetti, P.; Qutubuddin, S. *Thermochim. Acta* **2006**, *442*, 74–77.

8. Doh, J. G.; Cho, I. *Polym. Bull.* **1998**, *41*, 511–518.

9. Chieng, B. W.; Ibrahim, N. A.; Wan Yunus, W. M. Z. *Express Polym. Lett.* **2010**, *7*, 404–414.

10. Cheng, H. Y.; Weng, C. J.; Liou, S. J.; Yeh, J. M.; Liu, S. P. *Polym. Composite* **2010**, *31*, 2049–2056.

11. Mansoori, Y.; Atghia, S. V.; Zamanloo, M. R., Imanzadeh, G. H.; Sirousazar, M. *Eur. Polym. J.* **2010**, *46*, 1844–1853.

12. Jaymand, M. *J. Polym. Res.* **2011**, *18*, 957–963.

13. Yenice, Z.; Tasdelen, A. M.; Oral, A.; Guler, C.; Yagcı Y. *J. Polym. Sci., Pol. Chem.* **2009**, *47*, 2190–2197.

14. Safiullah, S. M.; Wasi, K. A.; Basha, K. A. *J. Coat. Technol. Res.* **2014**, *11*, 685–696.

15. Delibaş, A.; Soykan, C. *J. Macromol. Sci. A.* **2007**, *44*, 969–975.

16. Soykan, C.; Delibaş, A.; Coşkun, R. *Express Polym. Lett.* **2007**, *1*, 594–603.

17. Oral, A.; Tasdelen, M. A.; Demirel, A. L.; Yagcı, Y. *Polymer* **2009**, *50*, 3905–3910.

18. Orhan, T.; Isitman, N. A.; Hacaloglu, J.; Kaynak, C.; *Polym. Degrad. Stab.* **2012**, *97*, 273–280.

19. Helvacıoglu, E.; Aydın, V.; Nugay, T.; Nugay, N.; Uluocak, B. G.; Şen, S. *J. Poly. Res.* **2011**, *18*, 2341–2350.

20. Deopura, B. L.; Alagirusamy, R.; Joshi, M.; Gupta, B. *Polyesters and Polyamides*; Woodhead Publishing Limited and CRC Press, Boca Raton, FL, USA, 2008.

21. Thuc, C. N. H.; Grillet, A. C.; Reinert, L.; Ohashi, F.; Thuc, H. H.; Duclaux, L. *App. Clay Sci.* **2010**, *49*, 229–238.

22. He, H.; Ma, Y.; Zhu, J.; Yuan, P.; Qing, Y. *App. Clay. Sci.* **2010**, *48*, 67–72.

23. Sur, G. S.; Sun, H. L.; Lyu, S. G.; Mark, J. E. *Polymer* **2001**, *42*, 9783–9789.

24. Tyagi, B.; Chudasama, C. D.; Jasra, R. V. *Spectrochim. Acta A.* **2006**, *64*, 273–278.

25. Çelik, M.; Önal, M. *J. Appl. Polym. Sci.* **2004**, *94*, 1532–1538.

26. Yılmaz, O. *Prog. Org. Coat.* **2014**, *77*, 110–117.

27. Sapalidis, A. A.; Katsaros, F. K.; Kanellopoulos, N. K. In *PVA/Montmorillonite Nanocomposites: Development and Properties, Nanocomposites and Polymers with Analytical Methods*; Cuppoletti, J., Ed. InTech, 2011, pp. 29–50.

28. Van Herk, A. M.; *Macromol. Theory Simul.* **2000**, *9*, 433–441.

29. Bruice, P. Y. *Organic Chemistry*; 4th Edition, Pearson Prentice Hall, USA, 2004.

30. Toprakezer F. MSc Thesis, Çukurova University, Turkey, 2009.

31. Boyd, S. A.; Mortland, M. M.; Chiou, C. T. *Soil Sci. Soc. Am. J.* **1988**, *52*, 652–657.

32. Yalçınkaya, S. E.; Yıldız, N.; Saçak, M.; Çalımlı, A. *Turk. J. Chem.* **2010**, *34*, 581–592.